Microwave Spectrum of $N^{14}O^{16}$†

J. J. GALLAGHER, F. D. BEDARD, AND C. M. JOHNSON
Radiation Laboratory, The John Hopkins University, Baltimore, Maryland
(Received October 5, 1953)

The $J=1/2\rightarrow 3/2$ ($v=0$) rotational transition of the $^2\pi_{1/2}$ state of $N^{14}O^{16}$ has been measured. This transition occurs at 150 372.30 Mc/sec and is split into two groups of five lines due to Λ-type doubling and a large magnetic hyperfine interaction. The value of B_0 is found to be 1.69510 cm^{-1} and $r_0=1.1539$A. The Λ-doubling constant p is determined as 355.2 Mc/sec, and a spin of 1 is again confirmed for N^{14}. A preliminary analysis of the magnetic hyperfine structure is given, based on the interaction Hamiltonian $aI_{z'}L_{z'}+b\mathbf{I}\cdot\mathbf{S}+cI_{z'}S_{z'}$, where a, b, and c are constants.

INTRODUCTION

NITRIC oxide, quite unlike the usual molecule observed in the microwave region, has both electron spin and orbital angular momentum different from zero in its ground state. From optical spectra this ground state is known to be a $^2\Pi_{\frac{1}{2},\frac{3}{2}}$ with the $^2\Pi_{\frac{1}{2}}$ levels lying lower in energy. Also, since the doublet separation[1] is large (124.2 cm^{-1}) compared to the separations of the rotational energy levels (5 cm^{-1}), Hund's case (a) best describes the coupling of the various angular momentum vectors of the molecule. In the $^2\Pi_{\frac{1}{2}}$ state, which is the one of interest here, the spin and orbital angular momentum vectors are coupled to the internuclear axis with their components along this axis opposed. A net axial angular momentum $\mathbf{\Omega}$ of $\frac{1}{2}\hbar$ results which is combined vectorially with the angular momentum $\mathbf{N}$ due to rotation of the molecule to give the total angular momentum $\mathbf{J}$ (exclusive of nuclear spin). Figure 1 shows the arrangement of these vectors. Since Ω is a component of $\mathbf{J}$, it follows that for this case J cannot be less than $\frac{1}{2}$, and the rotational transitions, neglecting centrifugal stretching, occur between energy terms of the form:

$$F_v(J)=B_vJ(J+1)+(A-B)\Omega^2, \quad (1)$$

where B_v is the usual constant related to the molecular moment of inertia, I_v, by

$$B_v=h/8\pi^2cI_v, \quad (2)$$

and A is a constant (defined later) for a given electronic state. With the selection rule $\Delta J=0, \pm 1$ and $\Delta\Omega=0$ holding, it follows that a series of transitions similar to that for a diatomic molecule in a $^1\Sigma$ state is obtained. However, for the $^2\Pi_{\frac{1}{2}}$ case, the J values are half-integers and the lowest transition, which is the one observed in this experiment, is the $J=1/2\rightarrow 3/2$.

When $\Omega\neq 0$ each of the rotational energy levels given by Eq. (1) is doubly degenerate. However, due to the interaction of the electronic angular momentum with the rotational motion, this degeneracy is broken down, and each J level is split into two components of slightly different energy. This splitting known as Λ doubling (Ω doubling) increases with increasing J, thus causing two lines of slightly different frequency for each rotational transition.

The spectrum of $N^{14}O^{16}$ is further complicated by the nuclear spin of N^{14}. A nuclear magnetic moment is associated with this spin and serves to couple the nuclear spin $\mathbf{I}$ to the angular momentum vector $\mathbf{J}$ to give the resultant $\mathbf{F}$. The vector $\mathbf{F}$ can take values $(J+I)$, $(J+I-1)$, $\cdots|J-I|$, and, since each combination is of slightly different energy, the Λ-doublet components are split into a hyperfine pattern.

Nitric oxide is one of the very few molecules in which Λ doubling and magnetic hyperfine structure can be studied under the high resolution of microwave spectroscopy. It is the purpose of this paper to describe the observed spectrum[2] of the $J=1/2\rightarrow 3/2(v=0)$ transition of the $^2\Pi_{\frac{1}{2}}$ state of $N^{14}O^{16}$ and to give a preliminary correlation of the data with existing theory.

MEASUREMENTS AND APPARATUS

The $J=1/2\rightarrow 3/2$ transition occurs at approximately 2-mm wavelength, and the spectrum consists of ten lines split into two groups of five each. In the group occurring

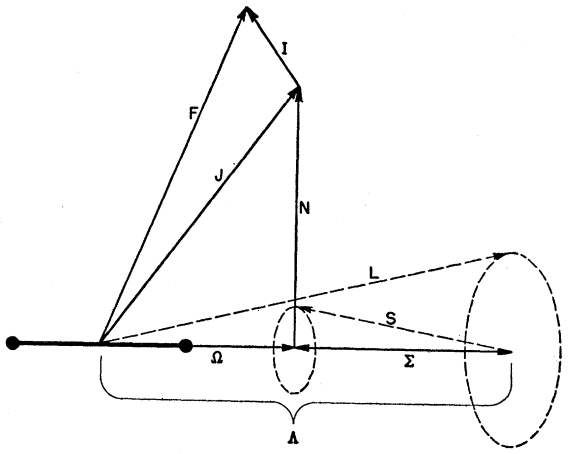

FIG. 1. Vector diagram for Hund's case (a) for the $^2\Pi_{1/2}$ state of $N^{14}O^{16}$.

† This research was supported by the U. S. Navy, Bureau of Ordnance.

[1] R. H. Gillette and E. H. Eyster, Phys. Rev. **56**, 1113 (1939).

[2] It was learned during the course of this work that these lines had also been found by Dr. Walter Gordy's group at Duke University.

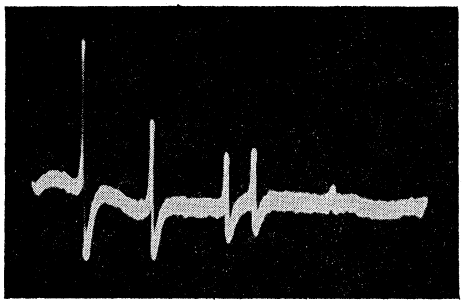

FIG. 2. Oscilloscope picture of the branch 1 lines of the $J=1/2\rightarrow3/2$ rotational transition of $N^{14}O^{16}$.

at the lower frequency, the $F=3/2\rightarrow1/2$ line is at the high-frequency end, and the $F=3/2\rightarrow5/2$ line is at the low-frequency end with a total separation of 69.1 Mc/sec. Somewhat surprisingly, this group bears little similarity to the other group at a slightly higher frequency. The separations between the components of this higher-frequency group are much larger with a total spread between end lines of 269.1 Mc/sec. Also, in contrast to the other case, the $F=3/2\rightarrow1/2$ line lies at the low-frequency end, and the $F=3/2\rightarrow5/2$ line occurs at the center of the group. Thus, the $F=3/2\rightarrow1/2$ transitions of the two groups lie closest together and are separated by 129.6 Mc/sec. These assignments were made on the basis of observed intensities. Although accurate intensity measurements even on a relative basis are difficult to make in microwave spectroscopy, there was no difficulty in the case of the $F=3/2\rightarrow1/2$ and $F=3/2\rightarrow5/2$ lines, since these two are the weakest and strongest, respectively, and differ by a factor of 25. All the other lines are about 30 to 40 percent as strong as the $F=3/2\rightarrow5/2$ line. Hereafter, the lines of the low-frequency group will be referred to as branch 1 and those of the high-frequency group as branch 2.

Figure 2 shows an oscilloscope picture of the five lines of branch 1. The lines of branch 2 were of comparable strengths, but were too widely spaced to be displayed together on the oscilloscope.

Table I gives the frequencies of all the lines, and Fig. 3 shows the complete spectrum and energy level diagram of the $J=1/2\rightarrow3/2$ transition. At this time the absolute frequencies of the lines have been measured only with a cavity wavemeter which had been calibrated on known absorption lines. Considerably greater accuracy will be obtained when precision measurements are made on the lines with a frequency standard.* The difference frequencies of the individual lines were measured by mixing the energy from a stabilized local-oscillator with a small portion of the power from the swept klystron. A marker was obtained by introducing the mixed output of the two oscillators into a communication receiver tuned to a frequency coinciding with the difference frequency of the klystrons at some point within the sweep range. When the output of the receiver was applied to the oscilloscope, a pip was produced each time the difference frequency coincided with the receiver frequency. This marker pip could be moved from one absorption peak to another by tuning the receiver, and the frequency separation of two lines was given directly by the difference in the receiver dial readings. All frequency separations, except the interval between the two groups, were also checked by producing sidebands on the klystron local oscillator with a variable-frequency (1 to 20 Mc/sec) oscillator. These sidebands were adjusted to coincide with a pair of lines, and the line separation was then given directly by the reading of the variable frequency oscillator.

Both the receiver and variable-frequency oscillator were calibrated with a crystal-controlled oscillator at the time of the measurements.

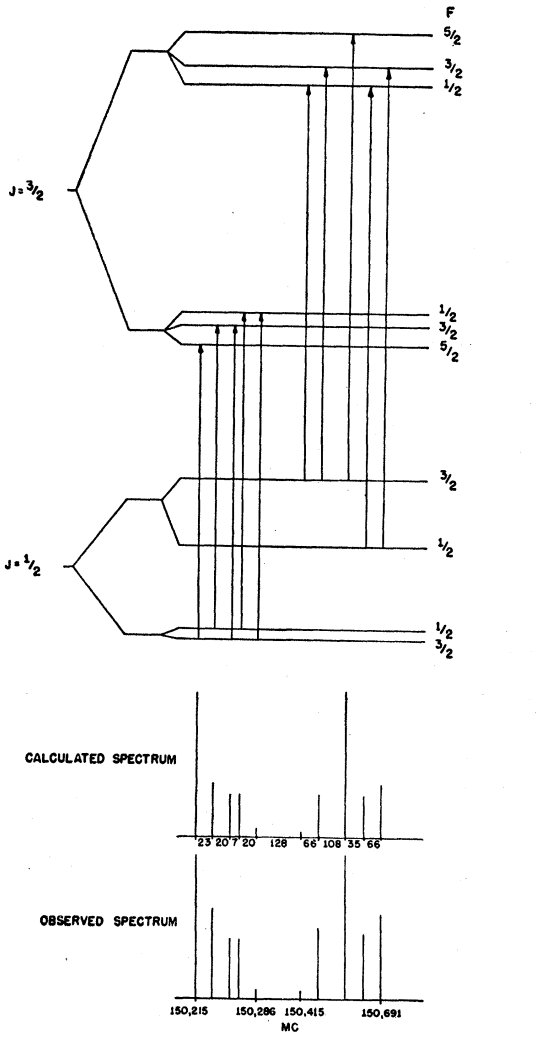

FIG. 3. Energy level diagram and complete spectrum of the $J=1/2\rightarrow3/2$ rotational transition of the $^2\Pi_{1/2}$ state of $N^{14}O^{16}$.

* Our frequency standard has been completed since this paper was submitted, and the measurements given here have been made using this standard rather than the less accurate method mentioned above.

TABLE I. Observed and calculated lines for the $J=1/2\rightarrow3/2$ transition of the $^2\Pi_{1/2}$ state of $N^{14}O^{16}$.

Transition	Measured frequency Absolute Mc/sec	Line separations Mc/sec	Calculated line separations Mc/sec	Relative intensities Measured	Calculated
Branch 1					
$F=3/2\rightarrow5/2$	150 176.30±0.25			100	100
		22.22	24.21		
$F=1/2\rightarrow3/2$	150 198.52			65	37.1
		20.05	19.98		
$F=3/2\rightarrow3/2$	150 218.57			43	29.6
		6.90	6.53		
$F=1/2\rightarrow1/2$	150 225.47			43	29.6
		19.91	19.98		
$F=3/2\rightarrow1/2$	150 245.38			5	3.7
Branch 2		129.64			
$F=3/2\rightarrow1/2$	150 375.02			5	3.7
		63.90	63.55		
$F=3/2\rightarrow3/2$	150 438.92			50	29.6
		107.33	105.91		
$F=3/2\rightarrow5/2$	150 546.25			100	100
		34.13	35.71		
$F=1/2\rightarrow1/2$	150 580.38			40	29.6
		63.73	63.55		
$F=1/2\rightarrow3/2$	150 644.11			60	37.1

The microwave energy at 150 kMc/sec (2-mm wavelength) was obtained by employing a silicon crystal multiplier to generate the fifth harmonic of the output of a 30-kMc/sec reflex klystron. For detection, a silicon crystal rectifier was also used. In both the multiplier and the detector, the cat whisker and crystal were mounted inside the wave guide as an integral part of the unit.

The absorption cell containing the NO gas was a seven-foot length of silver wave guide 0.280 in.×0.140 in. in cross section. Since we wished to observe the lowest rotational transition in the $^2\Pi_{\frac{1}{2}}$ state, a considerable increase in absorption intensity could be obtained by cooling the gas. The freezing point of NO is −163.6°C, and it still has a considerable vapor pressure at liquid nitrogen temperature. Therefore, the cell was enclosed in a one-inch diameter brass tube insulated with two inches of Styrofoam and kept immersed in liquid nitrogen during these measurements.

At this low temperature the lines were strong enough to be observed under high resolution with a simple video receiver. The $F=3/2\rightarrow1/2$ line, which is only about four percent as strong as the $F=3/2\rightarrow5/2$ line, appeared as a pip about three times noise when the tuning was optimized on its frequency.

INTERPRETATION OF DATA

Equation (1) is not a sufficiently accurate expression for the rotational energy levels when the measurements are made in the microwave region. The effect of rotational distortion on the spin multiplet must be included. Because of this interaction, the off-diagonal matrix elements belonging to pairs of rotational levels in different multiplet components are significant, and the expression for the rotational energy levels of the doublet becomes[3]

$$F_v(J)=B_v[(J+\tfrac{1}{2})^2-\Lambda^2]\pm\tfrac{1}{2}[4B_v^2(J+\tfrac{1}{2})^2+A\Lambda^2(A-4B_v)]^{\frac{1}{2}}+D_vJ^2(J+1)^2. \quad (3)$$

Here A and B_v are the same constants as in Eq. (1), and D_v is the centrifugal stretching constant. The constant A is a measure of the coupling between the electron spin S and the orbital angular momentum Λ. For large A/B_v, which holds for our case ($A/B_v\approx75$), Eq. (3) reduces to

$$F_v(J)=B_v\left(1\pm\frac{B_v}{\Lambda^2A}+\cdots\right)J(J+1)-D_vJ^2(J+1)^2, \quad (4)$$

where terms independent of J have been omitted. The (−) sign goes with the $^2\Pi_{\frac{1}{2}}$ component and thus, for the ground vibrational state of this case,

$$F_0(J)=B_{0\ \mathrm{eff}}J(J+1)-D_0J^2(J+1)^2, \quad (5)$$

where

$$B_{0\ \mathrm{eff}}=B_0(1-B_0/A), \quad (6)$$

and the frequency of the rotational transitions is given by

$$\nu_0=F_0(J+1)-F_0(J)=2B_{0\ \mathrm{eff}}(J+1)-4D_0(J+1)^3. \quad (7)$$

Each of the energy levels of Eq. (5) is split into two components since the symmetric and antisymmetric Λ-doubling states are not degenerate in a rotating molecule. Van Vleck[4] has calculated the perturbing matrix elements due to the components of electronic angular momentum perpendicular to the internuclear axis and has shown that the splitting of an energy level

[3] E. Hill and J. H. Van Vleck, Phys. Rev. **32**, 250 (1928).
[4] J. H. Van Vleck, Phys. Rev. **33**, 467 (1929).

in a $^2\Pi_{\frac{1}{2}}$ state due to Λ-type doubling is given by

$$F_c(J)-F_d(J)=p(J+\tfrac{1}{2}), \quad (8)$$

where

$$p\approx 4AB/\nu(\Pi\rightarrow\Sigma). \quad (9)$$

The subscript 0 has been dropped from the $F(J)$, and the new subscripts c and d are the usual spectroscopic notation for the levels of the Λ doublet. The frequency separation of the Λ-doublet lines is given by

$$\Delta\nu_\Lambda=[F_c(J+1)-F_c(J)]-[F_d(J+1)-(J)], \quad (10)$$

and, if Eq. 8 is substituted into this expression, then for any transition

$$\Delta\nu_\Lambda=p. \quad (11)$$

Van Vleck[4] has also shown theoretically that for small J values the Λ doubling in the $^2\Pi_{\frac{1}{2}}$ state is much greater than in the $^2\Pi_{\frac{3}{2}}$ state. Mulliken and Christy[5] have verified this difference experimentally, giving a value of 0.01 cm^{-1} (300 Mc/sec) for p or $\Delta\nu_\Lambda$ in the $^2\Pi_{\frac{1}{2}}$ state and a negligible splitting for the $^2\Pi_{\frac{3}{2}}$ state. Beringer and Rawson[6] in their work on the Zeeman transitions of NO have recently resolved Λ doubling in the $^2\Pi_{\frac{3}{2}}$ state and give a value of about 1.7 Mc/sec for the splitting.

The value of the splitting $\Delta\nu_\Lambda$, as well as the absolute frequencies of the Λ-doublet transitions ν_1 and ν_2, can be determined from Eqs. (24) and (25) that follow. Thus, from our data,

$$\Delta\nu_\Lambda=p=355.2 \text{ Mc/sec},$$
$$\nu_1=150\,194.70 \text{ Mc/sec},$$

and

$$\nu_2=150\,549.90 \text{ Mc/sec}$$

before hyperfine splitting.

If values of $D_0=0.53\times10^{-6}$ cm^{-1}, $A=124.2$ cm^{-1}, and $\alpha_e=0.0178$ cm^{-1} are taken from Gillette and Eyster,[1] then $B_{0\,\text{eff}}$ and B_0 can be determined from Eqs. (6) and (7) and B_e from the relation:

$$B_e=B_0+\tfrac{1}{2}\alpha_e. \quad (12)$$

Table II contains all the molecular parameters determined wholly or partially from this experiment. Our value of $B_0=1.69510$ cm^{-1} agrees quite well with the value 1.6957 cm^{-1} determined by Gillette and Eyster.[1]

It is well established that the nuclear spin of N^{14} is 1, and this experiment offers an additional verification of this value. Each of the Λ-doublet components was observed to be split into five lines. Any value of spin greater than one coupled to the angular momentum vector **J** would have produced six lines for the $J=1/2\rightarrow3/2$ transition. Nuclei with spins 1/2 or 0 would have given rise to three lines, and one line, respectively.

TABLE II. Molecular constants $N^{14}O^{16}$.

ν_0	150 372.30 Mc/sec
p	355.2 Mc/sec
$B_{0\text{eff}}$	50 124.17 Mc/sec = 1.67196 cm^{-1}
B_0	50 817.73 Mc/sec = 1.69510 cm^{-1}
I_0	16.5089×10^{-40} gm-cm^2
r_0	1.1539A
B_e	1.70400 cm^{-1} = 51 084.5 Mc/sec
I_e	16.4226×10^{-40} gm-cm^2
r_e	1.1509A

The quadrupole coupling constant of N^{14} in NO has been determined previously by Beringer and Castle[7] as approximately -1.7 Mc/sec. When the hyperfine splitting for the $J=1/2\rightarrow3/2$ transition of NO is calculated from such a coupling value, it comes out orders of magnitude smaller than the separations observed here.

The only other known mechanism available for coupling the nuclear spin to the angular momentum **J** is the interaction of the nuclear magnetic moment with the electronic orbital and spin magnetic moments. (The splitting due to interaction of the nuclear magnetic moment with the magnetic moment associated with the rotating nuclei is, in all cases previously examined by microwaves, much smaller than that due to quadrupole coupling.)

In the analysis presented here, the work of Frosch and Foley[8] on magnetic hyperfine structure will be employed. These authors derive the magnetic hyperfine interaction for a diatomic molecule from the Dirac equation of an electron in the field of the nucleus. After performing a series of unitary transformations on the Dirac equation and retaining only matrix elements diagonal in Λ, they arrive at the expression,

$$H=aI_{z'}L_{z'}+b\mathbf{I}\cdot\mathbf{S}+cI_{z'}S_{z'}, \quad (13)$$

for the magnetic hyperfine interaction Hamiltonian. The z' direction is along the internuclear axis, and

$$a=2g_I\mu_0\mu_N(1/r_1^3)_{\text{Av}},$$
$$b=2g_I\mu_0\mu_N\left[\frac{2}{3}\frac{\delta(r_1)}{r_1^2}-\frac{3\cos^2\chi-1}{2r_1^3}\right]_{\text{Av}}, \quad (14)$$
$$c=2g_I\mu_0\mu_N\left[\frac{3\cos^2\chi-1}{r_1^3}\right]_{\text{Av}}.$$

Here, r_1 is the distance from the nucleus with the spin to the electron, χ is the angle between r_1 and the internuclear axis, g_I the nuclear g factor, μ_N the nuclear magneton, μ_0 the Bohr magneton and $\delta(r_1)$ a coefficient that arises because of the quasi-relativistic treatment.

The quantities in brackets $[\ ]_{\text{Av}}$ are to be averaged over the electronic space coordinates for the particular state.

Equation (13) holds for both Hund's case (a) and case (b) and may be written

$$H=aI_{z'}L_{z'}+b(I_{x'}S_{x'}+I_{y'}S_{y'})+(b+c)I_{z'}S_{z'}. \quad (15)$$

[5] R. S. Mulliken and A. Christy, Phys. Rev. **38**, 87 (1931).
[6] R. A. Beringer and E. B. Rawson, Phys. Rev. **86**, 607 (1952).
[7] R. A. Beringer and J. G. Castle, Jr., Phys. Rev. **78**, 581 (1950).
[8] R. A. Frosch and H. M. Foley, Phys. Rev. **88**, 1337 (1952).

For a good case (a) molecule, the second term has only nonzero matrix elements which are off-diagonal in Λ and can be neglected. Hence,

$$H=[a\Lambda+(b+c)\Sigma]I_{z'}.$$

When Λ doubling is taken into account by considering the effect of matrix elements nondiagonal in Λ, Frosch and Foley obtain

$$W_{S/A}=(+|H|+)\pm(+|H|-) \tag{16}$$

for the hyperfine energy perturbations of the symmetric and antisymmetric Λ-doublet components of a case (a) $^2\Pi_{\frac{1}{2}}$ state.

Here,

$$(+|H|+)=D\frac{\mathbf{I}\cdot\mathbf{J}}{2J(J+1)}$$

$$=D\frac{F(F+1)-J(J+1)-I(I+1)}{4J(J+1)}, \tag{17}$$

where

$$D=[a\Lambda+(b+c)\Sigma]=a-(b+c)/2, \tag{18}$$

and

$$(+|H|-)=d(J+\tfrac{1}{2})\frac{F(F+1)-J(J+1)-I(I+1)}{4J(J+1)} \tag{19}$$

where

$$d=\frac{g_I\mu_0\mu_N}{2}\left[\frac{3}{r_1^3}\sin^2\chi\right]_{Av}. \tag{20}$$

The symmetric and antisymmetric Λ-doubling states are linear combinations of the degenerate electronic wave functions; i.e.,

$$(\psi_e)_S=[f(\Lambda,\Sigma)+f(-\Lambda,-\Sigma)](\tfrac{1}{2})^{\frac{1}{2}}, \tag{21}$$

$$(\psi_e)_A=[f(\Lambda,\Sigma)-f(-\Lambda,-\Sigma)](\tfrac{1}{2})^{\frac{1}{2}}. \tag{22}$$

As mentioned in the discussion of Λ doubling, these states have different interaction energies with the rotational motion thus causing each rotational level to be split into two components. Since for symmetry considerations the total wave function of a state can be written as a product,

$$\psi_{\text{total}}=\psi_e\psi_V\psi_R; \tag{23}$$

one of these component levels is positive (ψ_{total} symmetric) and one negative (ψ_{total} antisymmetric). The vibrational wave function, ψ_V, is always symmetric, and ψ_R is alternately symmetric and antisymmetric; therefore, $(\psi_e)_S$ will be the + component of one rotational level and − component of the next and likewise for $(\psi_e)_A$. Transitions occur only between + and − levels. Thus, the levels with ψ_e symmetric form one series and those with ψ_e antisymmetric form another series.

Since the constant d of Eq. (20) is positive ($g_I=+0.4$), the $(\psi_e)_A$ state must be the lower of the two components for each rotational state in order to fit the observed spectrum. Therefore, when the hyperfine perturbations of Eq. (16) are taken into account the line frequencies are given by

$$\nu=\nu_1+W_A(J=\tfrac{3}{2})-W_A(J=\tfrac{1}{2}) \tag{24}$$

for branch 1, and

$$\nu=\nu_2+W_S(J=\tfrac{3}{2})-W_S(J=\tfrac{1}{2}) \tag{25}$$

for branch 2. Here, ν_1 and ν_2 are the frequencies of the Λ-doublet lines without hyperfine splitting. Since the line separations were measured more accurately than the absolute frequencies, pairs of equations of the form (24) and/or (25) were solved in terms of the measured difference frequencies for the constants D and d as well as the Λ-doublet constant p. These constants are, of course, overdetermined by this group of equations, and hence have to be adjusted for best fit. Values of $D=92.6$ Mc/sec and $d=112.6$ Mc/sec give the calculated difference frequencies listed in Table I. The agreement between the observed and calculated spectra is very good but not quite within the experimental error. This difference is thought to be due to the effect of nuclear quadrupole coupling. Upon completion of our frequency standard more accurate measurements will be made on these lines, from which it may be possible to determine the quadrupole coupling of N^{14} in this molecule.

The magnetic hyperfine parameters evaluated here will be used in a later paper to obtain information on the electronic structure of NO.

It is hoped that enough sensitivity at 250 kMc/sec can be attained to observe the $J=3/2\rightarrow5/2$ transition in both the $^2\Pi_{\frac{1}{2}}$ and $^2\Pi_{\frac{3}{2}}$ states. Also, a spectroscope to measure the Zeeman splitting is being planned.

We are indebted to Dr. C. H. Townes for pointing out an error in our interpretation of a symmetry condition in the work by Frosch and Foley.

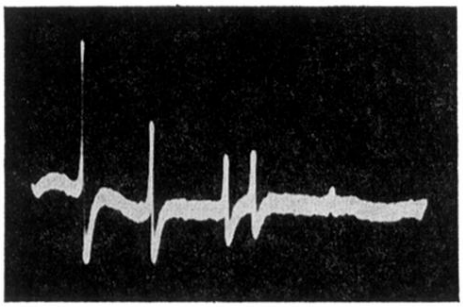

FIG. 2. Oscilloscope picture of the branch 1 lines of the $J=1/2\rightarrow 3/2$ rotational transition of $N^{14}O^{16}$.